Zeghloul A, Azzi A, Hasan A, Azzopardi BJ. Behavior and pressure drop of an upwardly two-phase flow through multi-hole orifices. Proceedings of the Institution of Mechanical Engineers, Part C: Journal of Mechanical Engineering Science. 2018;232(18):3281-3299. Copyright © IMechE 2017. DOI: 10.1177/0954406217736081

Behavior and pressure drop of an upwardly two-phase flow through multi-hole orifices

Ammar Zeghloul, Abdelwahid Azzi, Abbas H Hasan, Barry James Azzopardi

Abstract

Experimental results on hydrodynamic behavior and pressure drop of two-phase mixture flowing upwardly in a pipe containing single- and/or multi-hole orifice plate are presented. Time series of cross-sectionally averaged void fractions were measured using conductance probes at nine different axial locations along 34 mm internal diameter pipe. The measurements of upward single- and two-phase gas-liquid flow pressure drop across the orifices were achieved using accurate differential pressure transmitters. Four different layouts of orifices with different number of holes and positioning were used, providing that the opening area ratio (i.e. total area of the holes divided by the area of the pipe) and the thickness of all four orifices are identical. The four investigated orifices are; standard orifice, 4-holes square orifice, 4-hole triangular orifice and 9-holes square orifice respectively. It was found from the measurement of the void fraction upstream and downstream the orifices that the flow behavior is significantly affected by the layout of the orifice plate used. In addition, the flow starts to recover after approximately 7 D downstream the orifice. Furthermore, increasing orifice holes number results in decreasing the slip ratio. Standard deviation was used to identify the flow pattern before and after the orifices and found that the critical threshold transition occurred at a standard deviation of 0.2.

It was also inferred from the two-phase pressure drop data across the orifices that three different flow regimes, where the transition between bubbly-to-slug and slug-to-churn flow, can be identified. An assessment of the predicted two-phase flow multiplier using some of the existent models was achieved and found that the model proposed by Simpson et al. is the most reliable one. Single-phase pressure drop (which is independent on the liquid Reynolds number) was also measured and compared with correlations from literature.

Keywords: Multi-holes, void fraction, two-phase, pressure drop, upward

1. INTRODUCTION

Differential pressure (throttling) devices are widely used in single and multiphase flow applications. The most common differential pressure device is the orifice plate. Multi-hole orifice is a device that is increasingly used for the control and measurement of the flow in several industrial applications such as, oil and gas production, refrigeration, heat pump system and geothermal energy. Multi-hole orifice is a preferable device for a wide range of applications because it is easy to; manufacture, install and maintenance and it is relatively less expensive compared to other throttling devices. In addition, it shows good response to the flow with acceptable accuracy.

The multi-hole orifice is similar to the standard orifice plate but with multiple holes instead of just one single hole at the center of the plate. For multi-hole orifice, it is expected that the number, the diameter as well as the disposition of the holes, across the cross section of the plate, will affect significantly the flow behavior and the pressure drop across the orifice plate. One can cite another orifice plate, called slotted orifice. Unlike standard orifice plate, a slotted orifice plate consists of radial slots which cause the flow to disperse over the entire plate/pipe cross sectional area. This eliminates the swirling effects [1].

Considerable experimental and theoretical studies were conducted on multi-hole orifice in single phase flow. However, the behavior of multi-hole orifice in two-phase flow is still elusive and there have been very few studies reported in the literature. Several works have been carried out to understand the flow behavior and to study the pressure drop through a single hole orifice (standard orifice plate) for both single and two-phase flow. A review on this is given by the recent work of [2].

In single phase flows, an effort has been devoted to study, both experimentally and numerically, the behavior (e.g. the pressure drop) of the flow using multi-hole orifice [3-9]. Slotted orifice has also received a great deal of attention in the recent years; one can cite the work of Morrison et al. [10]. The above studies are briefly discussed below.

Kolodzie and Van Winkle [3] analyzed experimentally the effects of the design variables on the pressure drop across dry perforated plates used in a distillation column. These variables are pitch to hole diameter ratios, hole sizes, thickness of the plate, Reynolds number based on the hole diameter and number of the holes. For design purposes, they assumed that the pressure drop through or across the plates of the distillation column can be considered as a combination of two effects; the pressure drop due to the liquid head over the plate and the pressure drop due to the vapor discharge through a dry plate. From their study, they proposed a graphical correlation for orifice coefficient function of all the influencing design parameters. They reported that they found small deviations when comparing this correlation and data presented by other authors.

Gan and Riffat [4] carried out experimental tests, using air as a fluid, to determine the pressure loss coefficient for perforated plates (with 145 uniformly-spaced holes of 20mm diameter) and square edge orifice (with a diameter of 239 mm) in a square duct for different Reynolds numbers. They also used a CFD package (Fluent) to predict the pressure distribution on the orifice plate and to study the influence of the plate thickness on the pressure loss coefficient of the plate. They found that for a fixed free area ratio (i.e. the ratio of the total cross sectional area of the orifice to the cross sectional area of the duct) of 0.5, the pressure loss coefficient of a perforated plate in a square duct is higher than that of an orifice plate. For Reynolds number of 1.6×10^5 to 3.7×10^5 (i.e. turbulent flow), the effect of this number on the pressure loss coefficient is negligible. They concluded that, the pressure loss through an orifice plate can be reduced substantially when the plate thickness increases to 1.5 times the orifice diameter.

Malavasi et al. [11] studied, experimentally, the dependence of the pressure loss coefficient through different perforated plates on the geometrical parameters and flow variables (such as, the equivalent diameter ratio, the Reynolds number, the relative thickness of the plate, number of holes and the disposition of the holes). Water was used as a single phase fluid. They used perforated plates with; equivalent diameter ratio in the range of 0.2-0.72, relative hole thickness in the range of 0.2-1.44 and the hole numbers between 3 to 52. They found that a reduction in the equivalent diameter ratio leads to an increase in the pressure loss coefficient. In addition, they reported that the relative thickness of the plate has a significant effect on the pressure loss coefficient. Furthermore, the number of the holes and the disposition of the holes have noticeable effect in which if the number of the holes increases, the pressure loss coefficient decreases. They have attributed this reduction on the pressure loss coefficient to a reduction of the recirculation zones area (or size) between the holes.

Testud et al; [5] were interested in studying, experimentally, the cavitation phenomenon in single and multi-hole orifice under industrial conditions, i.e., with pressure drop varying from 3 to 30 bar and cavitation pressure from 0.03 to 0.74. Their experiments revealed that in the so-called developed cavitation regime, a multi-hole orifice was more silent than single-hole one with the same total cross sectional opening, and claimed that this might be partially explained by the absence of correlation between the sound produced by different holes in the absence of whistling.

Zhao et al. [6] carried out a detailed work on pressure loss through multi-hole orifice plate using water as a fluid. They investigated the influence of the key geometric parameters (i.e. the total orifice number n, the equivalent diameter ratio defined as $n^{0.5}d/D$ where d/D is the diameter ratio and the orifice distribution density D_d which is defined as, d_{hmin}/D, where d_{hmin} is the minimum spacing between the orifices edges located at adjacent center circles) on the pressure loss coefficient of the orifice plate. The investigated multi-hole orifices have a thickness of 2 mm and the total number of the holes varied from 3 to 13, some are centered while others are non-centered orifices with circular and rectangular arrangements. From these experiments, they derived two polynomial correlations for the pressure loss coefficient, ζ which are mainly depend on the equivalent diameter ratio, EDR and the diameter ratio of a single hole orifice, DR respectively. One finding worth to mention is that the pressure loss coefficient for multi-hole orifices is generally higher for those with fewer perforated holes.

Mayens et al. [7] conducted a series of experiments to study the pressure loss coefficient and the onset of cavitation generated by water flow through 16 perforated plates with varying thickness and flow area-to-pipe ratio. The total perforation hole area to the pipe area ratio is in the range of 0.11-0.6 and the ratio of the plate thickness to perforation hole diameter is between 0.25 and 3.3. The number of holes in the plates ranging from 4 to1800. The average fluid velocity is from 0.35 to 8.5 m/s. They found that the pressure loss coefficient, in general, decreased with increasing free-area ratio and increasing thickness to hole diameter ratio. In addition, with increasing free-area ratio, the critical cavitation and the cavitation number at the points of cavitation inception increases. However, the effects of varying the thickness-to-hole diameter ratio indicate that the cavitation number at inception shows a local maximum at the thickness-to-hole ratio between 0.5 and 1.0. They proposed an empirical model to predict the loss coefficient for perforated plate which was based on the free-area ratio and the thickness of the plate. The model showed good agreement with authors' data and with previous studies.

Barki et al. [8] analyzed fluid flow through a single hole and multi-hole orifice plates using Ansys Fluent commercial CFD code. They used single, four, nine and sixteen holes, with four diameter ratios, 0.6, 0.3, 0.2, and 0.15. The inner pipe diameter used was 50 mm and thickness of the plate was 3 mm. They concluded that pressure drop is minimum for multi-hole orifice plate compared to single hole plate. Pressure recovery for single hole orifice plates needed much longer straight pipe, whereas multi-hole orifice plate needed shorter pipe for pressure recovery. The fluid flow distribution is more steady and uniform for multi-hole orifice plate compared to a single hole plate.

Singh and Tharakan [9] studied, both experimentally and numerically, the flow characteristics of multi-hole orifice plates over a wide range of Reynolds numbers. They used one standard orifice plate (with a central circular orifice of 10.6 mm diameter and an open area ratio, β of 0.5) and 7 different multi-hole orifice plates (each with 8 holes and the diameter of the peripheral holes ranging from 2.81 to 3.3 mm). The Pitch circle diameter for peripheral holes ranging from 10 to 16 mm). The fluid (water) flow Reynolds number was varied from 500 to 20000. They found that the pressure recovery for multi-hole orifice plate is larger than the pressure recovery of the single-hole orifice plate with the same flow area. They have attributed this to the smaller size of eddies that can be generated immediately downstream of the orifice plates. They also reported that the discharge coefficient of multi-hole plates is larger than that of standard orifice (i.e. with a single hole at the center of the plate) over a wide range of Reynolds numbers.

Morrison et al. [10] studied and compared the performance of a standard orifice and a slotted plate (which consists of three concentric rings, each with several radial slots). They found that, with the same diameter ratio (i.e. β=0.5), the sensitivity to the upstream flow conditioning in slotted orifice plate is less than that in a standard orifice plate. They also studied the variation of the discharge coefficient with the inlet velocity with and without swirling flow. They reported that, the variation of the discharge coefficient with the inlet velocity, when there is no swirling flow, was -1% to 6% for the standard orifice plate and ±0.25% for the slotted plate. In the case of swirling flow, the variation of the discharge coefficient for the standard orifice was above 5% while it was below 2% for the slotted pate.

For two-phase flow, despite their possible advantages the muti-hole orifice has received less attention comparatively to a single-phase flow. To the best knowledge of the authors, the only work reported on the open literature are those of Alimonti et al. [13] on multi-hole orifice and those of Morrison et al. [12], Geng et al. [14], Pirouzpanah et al. [15] and Annamalai et al. [16] on slotted orifice plate. The above studies are briefly described below.

Alimonti et al. [13] reported results on frictional pressure drop and void fraction of the air-water two-phase bubbly and slug flow through multi-hole orifice valve (MOV). A Willis MOVs using three different sections of discs with throat thickness diameter ratios of; 1.41 (with 2 holes of 15 mm diameter), 1.66 (with 2 holes of 2.8 mm diameter) and 2.21 (with 2 holes of 9.6 mm diameter) and orifice thickness of 30 mm have been investigated. The flow rate was regulated by rotating one of the two discs over the other (i.e. fixed one) which in turns, changes the total orifice flow area. They concluded that the pressure drop multiplier data obtained experimentally from MOVs cannot be properly fitted and correlated with conventional correlations for the pressure drop multiplier. They attributed this error to the MOV geometric effects. Therefore, they developed a new correlation by modifying the constants of the two-phase flow pressure drop multiplier for an MOV and found that it fairly agreed with the conventional correlations. They also observed significant effects of geometry on the hydrodynamic characteristics of the flow in which at high velocity, the gas concentrates in the core vortex causing the boundary layer of the liquid flowing along the wall of the valve to be separated. In addition, they observed swirling flow that could be propagate several diameters away from the outlet of MOV.

Morrison et al. [12] analyzed the behavior of a slotted orifice flow meter (with an equivalent β-ratio of 0.50) in a stratified air-water flow using a horizontal 50.8 mm diameter acrylic pipe. They used the same experimental facility utilized by Morrison [10] but with injecting water upstream of the orifice plate. The air-water mass flow quality was varied from 1 to 0.2 by adding water to the air flow. The range of air Reynolds numbers was 18,000 to over 200,000 at a pipeline pressure of 101 kPa. They used a standard orifice flow meter mass flow rate equation to evaluate the performance of the slotted orifice plate at one pressure line (i.e. 101 kPa).

They plotted the factor KY (the product of the flow coefficient and the expansion factor), with the mass flow quality using the density of the gas and the water respectively and found that at a line pressure of 101 kPa, the factor KY is dependent only on the mass flow quality and independent of the air Reynolds numbers. This dependence of KY factor on the mass flow quality was monotonic, i.e. it increases as the mass flow quality decreases (and hence increasing in the water flow rate). They also noticed that the pressure drop across the slotted plate increases with increasing air Reynolds number and decreasing mass flow quality. In addition, the slotted orifice plate showed insensitive response to the upstream velocity profile. They concluded that a prior knowledge of the mass flow quality helps to determine KY factor. The later can then be used in conjunction with the density of the gas or water to estimate the two-phase mass flow rate.

Geng et al. [14] studied, numerically and experimentally, the single and two-phase flow (wet gas flow) through a standard and a slotted orifice plate with the same area ratio of 0.5. The slotted plate used has 48 rectangular slots (2x5.32 mm) positioned along three concentric circles. The thickness of the orifice was 3 mm. In this study, the velocity and density contours as well as the static pressure across the standard and the slotted orifice flow meter were analyzed. They have developed two new empirical correlations (as a function of the gas dimensionless Froude number and Lockhart-Martinelli parameter) for two-phase pressure drop multiplier across the slotted orifice. From the numerical simulation, they reported that the use of a slotted orifice showed some superior characteristics compared to the standard orifice plate such as, the pressure recovery requires a short pipeline; the velocity contour is more steady and uniform and there is no liquid accumulation upstream and downstream of the orifice in air-water mixture. Furthermore, their simulation surprisingly shows that the contours of static pressure of single phase and two-phase flow are similar with small difference. From experimental data, they found that the main three dominant parameters that affect the two-phase multiplier in a slotted orifice are, the pressure line, P; gas Froude number, Fr_g and the modified Lockhart-Martinelli parameter X. They observed that the lower the β ratio is, the more sensitive the slotted orifice will be to the presence of the liquid which is preferable for the wet gas metering applications. In contrast, they also found that the slotted orifice is less sensitive to the flow regime/pattern changes where the two-phase pressure drop multiplier in wavy flow is greater than that in mist or annular flow.

Pirouzpanah et al. [15] designed an air-water two-phase flow meter using a combination of the swirl flow meter and a slotted orifice plate in a coupled configuration. A slotted orifice (with β=0.467) is mainly used to homogenize the flow upstream the swirl flow meter. The response of this coupled system (i.e. the swirl flow meter and a slotted orifice plate) was tested using seven different liquid mass flow rate in the range of 108.8 to 353.8 kg/min, each with the gas volume fraction GVF from 0 to 100%. The diameter of the test section was 50.8 mm and the flow regime upstream the multiphase flow meter was slug flow. They observed that the quality of the two-phase flow homogeneity degraded gradually as the flow progressed downstream the slotted orifice plate and therefore, they suggested to implement a close coupled system to insure high quality of homogeneity upstream the swirl flow meter. The frequency output of the swirl flow meter was found to be repeatable in a wide range of GVF (60% to 95%) and the accuracy of the multiphase flow meter was ± 0.63%.

Recently, Annamali et al. [16] followed the work of Pirouzpanah by focusing on the homogenization phenomena of air-water two-phase flow mixture after passing the slotted orifice obstruction. They mainly studied how the relative homogeneity of the two-phase flow mixture varies downstream of the slotted orifice plate in a horizontal bubbly and slug flow regimes using electrical resistance tomography (ERT) technique. Electrodes were placed circumferentially around the pipe at 8 different planes along the pipe to measure the instantaneous localized concentration distribution across each plane. They found that the optimum downstream location from the slotted orifice where homogenization of two-phase flow mixture was optimum can be obtained at the distances from 1.5 to 2 times pipe diameter. Moreover, the slotted orifice plate has low sensitivity to the upstream flow condition.

The present work aims to study the hydrodynamic behavior and pressure drop of two-phase flows through four different orifice plates, namely; standard orifice, 4-holes square orifice, 4-hole triangular orifice and 9-holes square orifice (see Fig.2 for more details on orifice plate geometry).

2. EXPERIMENTAL SETUP AND THE METHODOLOGY

A schematic diagram of the experimental facility employed showing the locations of the orifice plates and nine conductance probes used for the void fraction measurements is shown in Fig.1. It is the same test facility as that used previously by Zeghloul et al. [17]. The main modification is the addition of the measurement devices for pressure drop and the associated pipes and fittings.

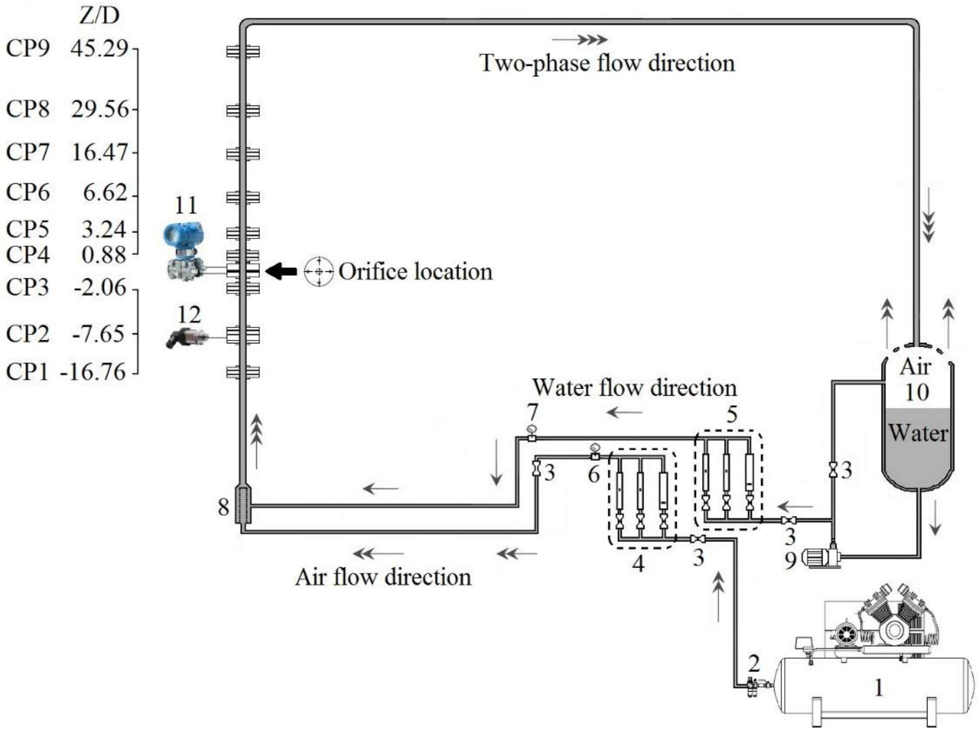

Fig. 1 Schematic diagram of the experimental facility

The orifice vertical test section was made of transparent acrylic resin, which permits visual observation of the flow pattern, is 6 m long with an internal diameter, *D*, of 34 mm and a wall thickness of 4 mm. Tap water is drawn by the pump from a storage tank, which also acts as a phase separator, and injected into the mixer where it is combined with the air supplied from the compressor.

The mixer made of Polyvinyl chloride (PVC) has a short concentric pipe, with 64 holes with 1 mm diameter spaced equally in 8 columns over a length of 80 mm on the cylindrical surface and with the top blanked off, as the gas injector. The liquid is introduced into the annular chamber surrounding this gas injector, creating thus, more even circumferential mixing.

Downstream of the mixer, the air-water mixture flows through the orifice vertical test section, a vertical bend, a horizontal pipe, finally through a final bend and down to the storage tank, where the air and the water are separated.

The water is recirculated and the air is released to the atmosphere. Inflow of air and water are controlled by valves and metered using one of banks of calibrated variable area meters mounted in parallel before the mixing unit. The maximum uncertainties in the liquid and gas flow rate measurements are 2 %. The static pressure of the air flow is measured prior entering the mixing section. A (0-100 °C) thermometer with an accuracy of 1 % of the full scale is used for temperature measurement. The temperature during the experiments was around 25°C. Tap water was used in the experiments. It had a conductivity of ~600 μS/cm (measured with a LUTRON YK-43C electrical conductivity meter). The electrical conductivity increases with temperature and these changes can affect the measured void fraction. To minimize changes in conductivity within the same experimental run, tap water was fed continuously to the storage tank and any excess was discharged to drain.

A series of four orifices have been used in the present study. Their dimensions are summarized in Table 1.

Table 1: Dimensions of the orifices

Orifice	Diameter, d [mm]	No. of holes	Thickness, t [mm]	Open area, $\sigma=A_h/A_p$	Thickness ratio, t/d
Standard orifice	18.5	1	1.9	0.30	0.1
4-holes square	9 mm	4	1.9		0.1
4-holes triangular	9 mm	4	1.9		0.1
9-holes square	6 mm	9	1.9		0.1

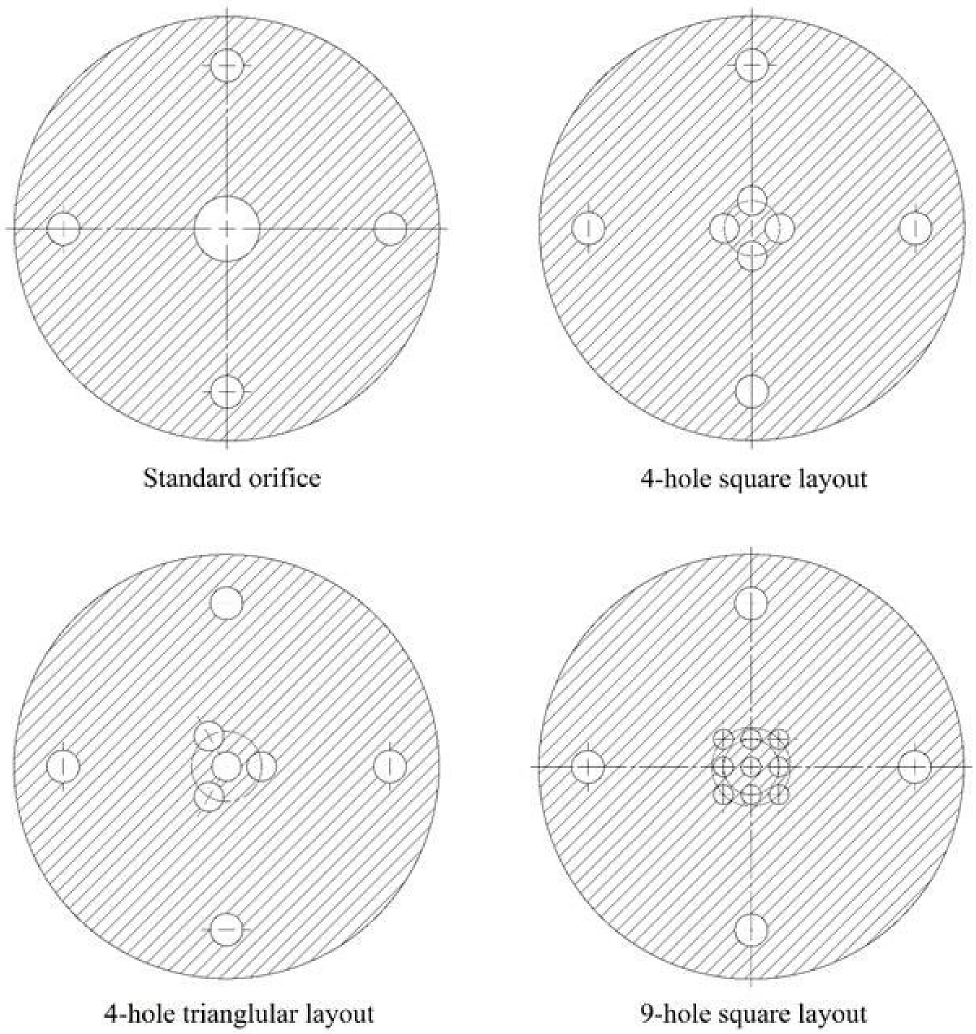

Figure 2: Four different layouts of orifice plates

In order to measure the average void fraction along the test section, nine ring-shaped plate conductance probes were installed. Three of these at 570, 260 and 70 mm before the orifice; and six probes at 30, 110, 225, 560, 1005 and 1335 mm after the orifice. The orifice is installed at 4110 mm (121 pipe diameters) downstream the mixer. Details on this technique are given in Zeghloul et al. [17].

The pressure drop across the orifice is measured by using two FOXBORO differential pressure transmitters mounted in parallel. The ranges of these two differential pressure transmitters are

(0-7.2 kPa) and (0-36 kPa) respectively, with an accuracy of 2 % of the full scale of these transmitters.

ISO 5167-1 [18] suggests that for the measurement of the pressure drop across the orifice, the pressure transmitter should be connected to tappings placed at 1*D* upstream and 0.5*D* downstream of the orifice plate.

To ensure accurate measurements of the pressure drop, a purging arrangement, illustrated in Fig. 3 was employed to ensure no air bubbles were present in the measuring pressure lines. The drain valves, V1 and V2, on either side of the diaphragm are firstly opened. With the pump switched on water flows in the pipe orifice test section and in the transparent plastic tubes leading to the differential pressure transmitter. If valves V3 and V4 are then opened water is forced out to the drain valves carrying bubbles with them. Once it is seen that all air has been removed, the four valves (V1 to V4) are closed and measurements are made.

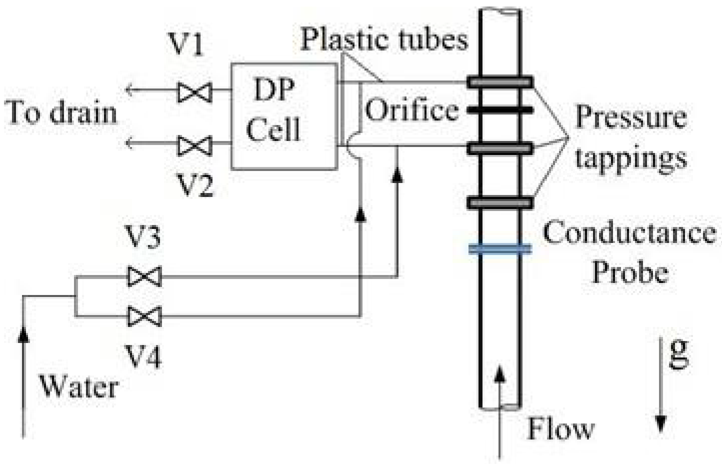

Fig. 3 Upward pressure drop measurement and purging system arrangements [2]

An absolute pressure transmitter (0-1.6 bar) made by IMPRESS Sensors and Systems Company with an accuracy of 0.1% of the full scale , was attached to a tapping 8*D* upstream of the orifice to measure the absolute pressure.

The output signals obtained from the electronic circuit associated with the conductance probes, along with those from the differential pressure transmitters as well as that from the absolute pressure transducer are sent to the data acquisition unit. The latter consists of a Personal Computer fitted with Data acquisition Card (12 bits NI DAQ card-6062E) employing LabView 8.6 software. Data is sampled at a frequency of 200 Hz over the period of 30 seconds.

3. Results

In the present study the superficial velocities of the air was between 0 and 0.4 m/s and that of the water between 0.3 and 0.91 m/s. Within these velocity ranges, single-phase flow, bubbly, slug and churn two-phase flow regimes were observed through the transparent vertical acrylic test section before the orifice.

3.1 Flow behavior

3.1.1 Void fraction time series before and after the orifices

Examples of time series of void fraction measured by conductance probe CP1 (upstream the orifices) and by three conductance probe CP4, CP5 and CP6 (downstream the orifices) for the three investigated flow regimes, bubbly, slug and churn flow, are shown in Fig. 4. It appears from this figure that the flow behavior is significantly affected by the layouts of the orifices. The standard orifice type affects greatly the flow behavior. For bubbly flow (4-1- (a)), there is a clear increase of the void fraction when the mixture passes through the orifice. This increase could be attributed to the coalescence phenomena due to the reduction of the flow section. It is seen that the flow starts to recover at the position of CP6 (i.e. after 7 D downstream the orifice plate) in which the variation of the void fraction becomes quite close to that recorded at CP1. This can also be clearly seen from fig.5(a). For churn flow (4-2-(a)), it seems that the flow is not greatly affected by the orifice as for bubbly flow. For slug flow at low gas and liquid flow rates (4-3-(a)), the variation of the void fraction (and hence the flow behavior) is greatly affected by the orifice layout used. The time series void fraction at CP4 is similar to that of bubbly flow regime which attempts to return to its initial shape from CP6, showing the characteristic signature of time series of a slug flow with its two distinct (palliers). For slug flow at high gas and medium liquid flow rates (4-4-(a)), the trend of the void fraction evolution is quite close to that of churn flow at CP4 and the flow is recovered at CP6.

The four holes, square and triangle layout orifices influences similarly to the standard orifice the behavior of the bubbly flow (4-1(b); 4-1(c)), however the flow starts to return to its initial shape from the CP5 and there is not great noticeable difference between these two-multi-hole orifices. For the nine hole square orifice (4-1-(d)), it seems, with the exception of a small increase in the average void fraction, that this geometry doesn't affect the flow behavior. The behavior of the Churn flow is slightly influences by the presence of the four holes orifices (4-2-b), (4-2-c), and the flow returns to its initial form from CP5; while practically no influence of the nine hole orifice on this flow is remarkable. For slug flow with low gas and liquid flow rates, the effects of the presence of the four holes orifices (4-3-b) and (4-3-c) are obvious. There is a break of the Taylor bubbles when passing through these obstructions; and similarly, to the standard orifice the void fraction time series shape is close to that of a bubbly flow. Moreover, the flow did not recover yet at CP6. Same observations can be made for the nine hole orifice with the exception that the flow is practically recovered at this latter probe. For slug flow with low high gas flow rate and medium liquid flow rate, similarly the effects of the presence of the four holes orifices and the nine hole orifice are obvious. The Taylor bubbles break up when passing through these orifices. At CP4 the shape of the void fraction time series is that of churn flow and the flow recovery starts practically from CP5.

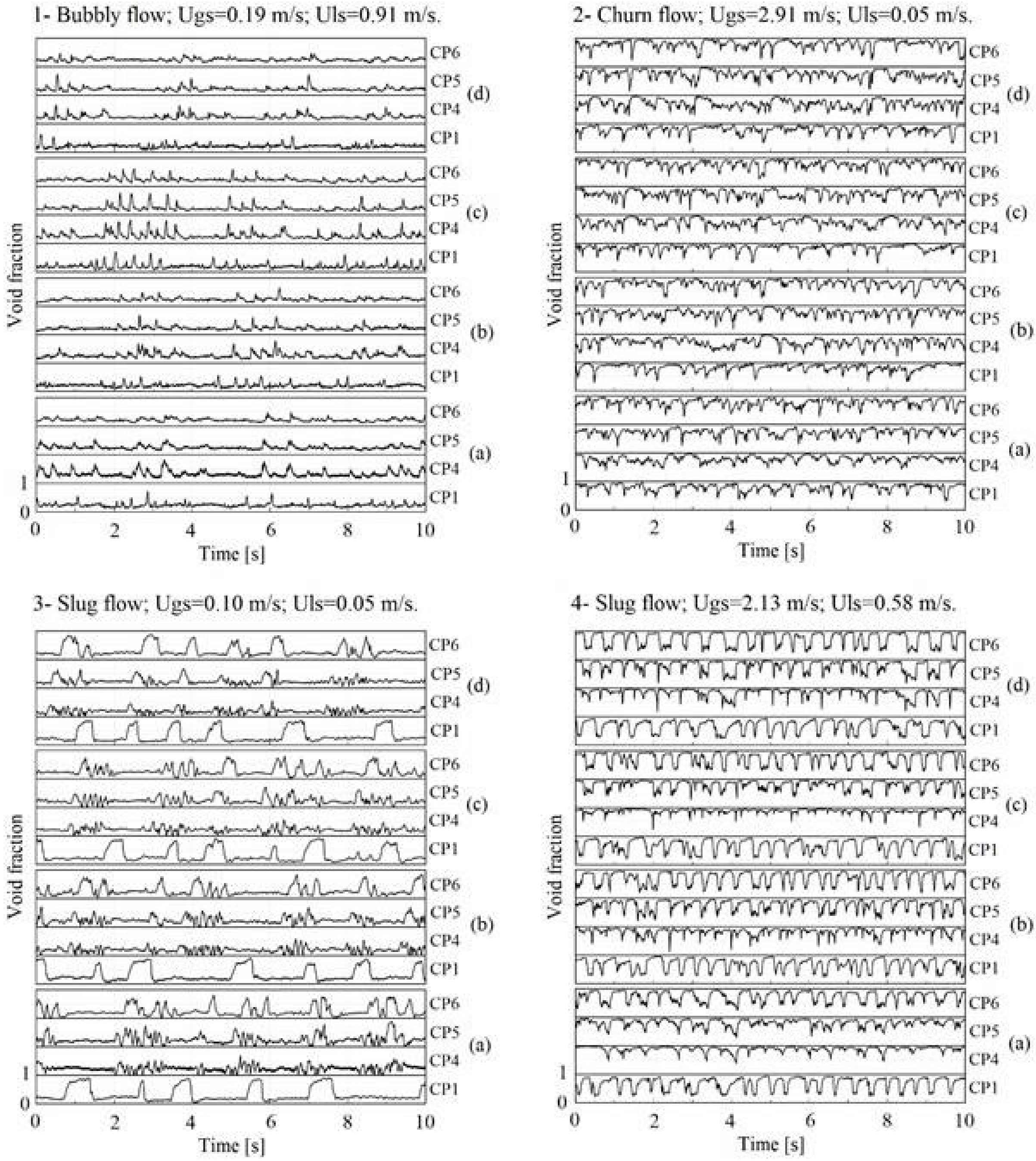

Fig. 4 Time series void fraction upstream and downstream orifices: a) standard orifice, b) four hole square layout, c) four hole triangle layout, d) nine hole square layout.

3.1.2 Axial evolution of the average void fraction upstream and downstream the orifices

An example of the evolution of the average void fraction along the test section upstream and downstream the standard and the three multi-hole orifices for different combinations of the gas and liquid superficial velocities is plotted in Fig. 5. It is clear that for bubbly flow (Fig. 5 (a)), the axial variation of the void fraction is different than that for the churn and slug flow regimes (Fig. 5 (b) (c) and (d)). For bubbly flow (Fig. 5 (a)) the time averaged void fraction is approximately constant upstream the orifice. Immediately after the orifice plate, a sharp increase of the void fraction (for all four orifice layouts) can be seen in which the standard orifice plate, among other layouts, showed the maximum peak of this increase. In contrast, the response of the nine hole square orifice plate showed the minimum increase in the void fraction. Its value has practically doubled. The increase in the void fraction results from the homogenizing effect due to the mixing. As the flow progresses along the pipe the average void fraction drops as the frothy mixture regain bubbly flow. The void fraction then increases (after CP6) and becomes approximately constant after CP7. This is due to the fact that the bubble size grow to a quasi-stable distribution.

For churn flow (Fig. 5 (b) and for all four investigated orifices an increase in the void fraction before orifice obstructions is obvious followed by a sharp decrease downstream of orifices. Then an increase in the void fraction occurred where the flow is approximately recovered after CP6.

For slug flow with low gas and liquid flow rates (Fig. 5 (c)), the void fraction just before the orifices increases sharply due to the constriction in the flow path. This increase is the highest for the standard orifice one. The void fraction then decreases dramatically after the orifices then increases once again to reach into its initial value almost at the sixth probe (CP6).

For slug flow with practically medium liquid and high gas flow rates, contrarily to the slug with low liquid and gas flow rates, there is an increase in the void fraction when passing through the orifices following by a decrease in which the flow is recovered almost after CP6.

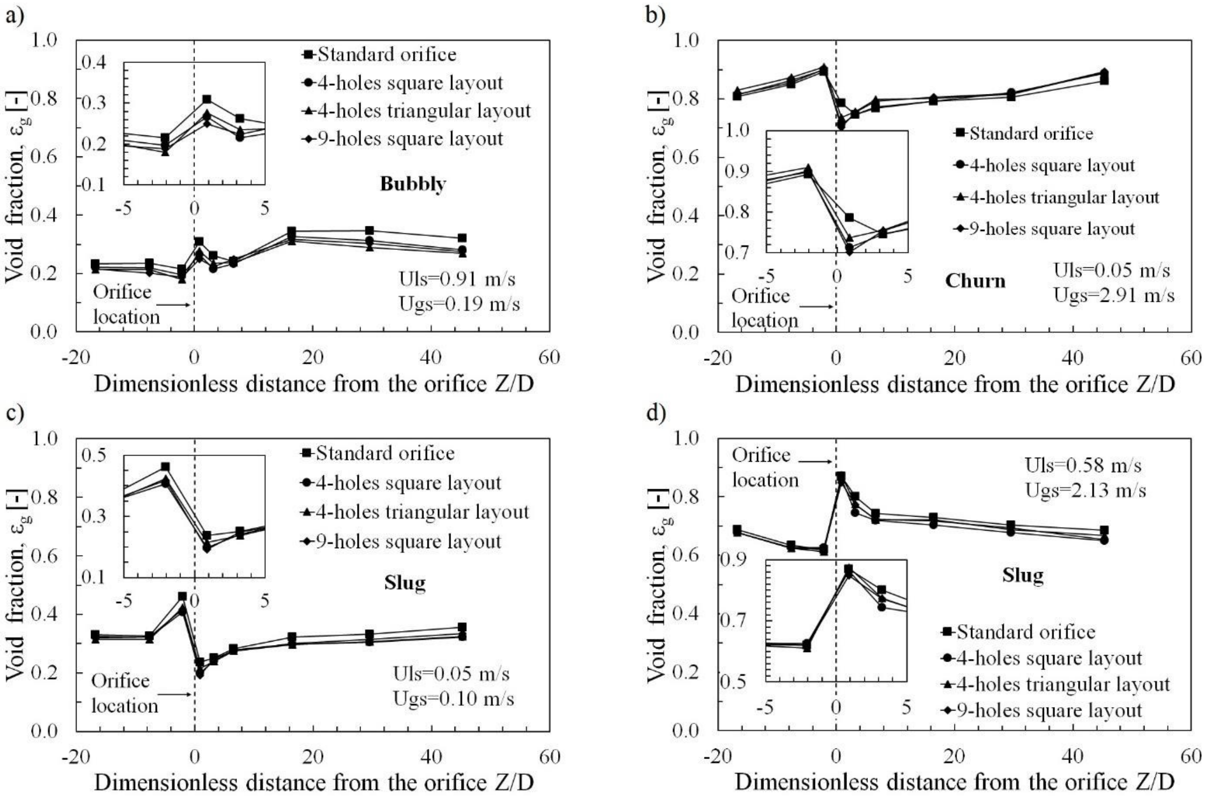

Fig. 5. Evolution of the average void fraction along the test section before and after the orifices for different gas and liquid superficial velocities combinations.

3.1.3 Standard deviation of the void fraction upstream and close downstream the orifices

In this section the statistical standard deviation parameter of the void fraction is used to identify the flow pattern before and after the orifices. This method has successfully been used by Kaji et al. [19] who reported that the Standard Deviation is a useful tool to identify slug flow.

They used 19 mm internal diameter pipe and found that a standard deviation of 0.1 can be used as a threshold line to identify the three main regimes; bubbly, slug and churn flow. In other words, they plotted a standard deviation, S_D versus superficial gas velocity, U_{gs} and divide it into three regions;

(i) bubbly flow, at low to moderate U_{gs} and S_D <0.1

(ii) slug flow, where S_D >0.1

(iii) churn flow, at moderate to high U_{gs} and S_D <0.1

The standard deviation is defined as;

$$S_D = \sqrt{\frac{\sum_{i=1}^{n} (\varepsilon_{gi} - \bar{\varepsilon}_g)^2}{n}} \qquad (1)$$

where n is the number of samples, ε_g and $\bar{\varepsilon_g}$ are the void fraction and the mean void fraction respectively.

Figure 6 shows the variation of the standard deviation of the void fraction measured upstream the orifice at CP 1 with the gas superficial velocity at different liquid superficial velocities. It is seen from Fig.6 that for the current work (where the pipe diameter is 34mm), the standard deviation threshold value is approximately 0.2. The vertical threshold line which indicates a transition between bubbly and slug flow regimes is approximately occurred at the gas superficial velocity of 0.7 m/s.

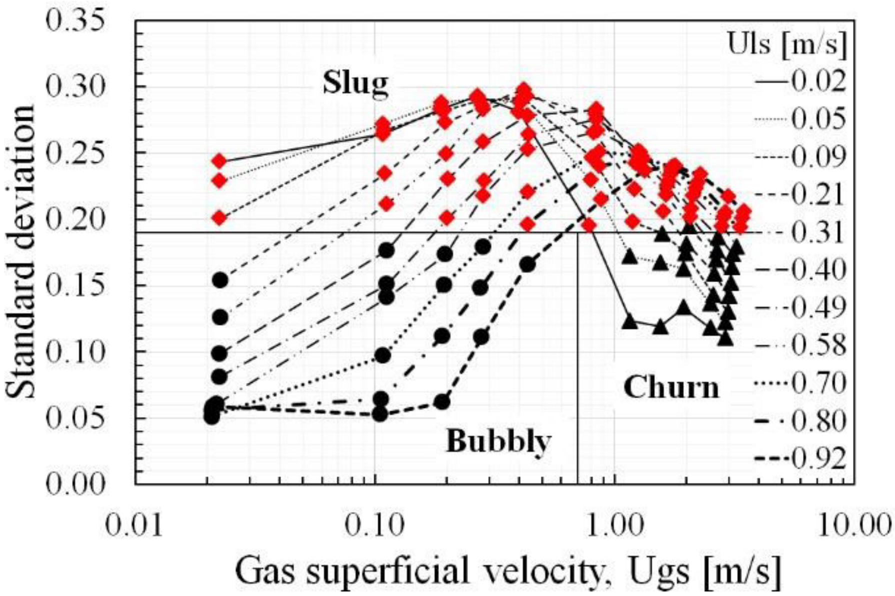

Fig.6. Flow pattern with void fraction standard deviation upstream the orifices at CP 1

In Fig.7, a sample of the time average void fraction and its standard deviation, are plotted versus the gas superficial velocity for different liquid superficial velocities, at conductance probes CP1, CP4 and CP5, using the standard orifice plate. For the lowest liquid superficial velocity U_{ls}=0.21 m/s, the standard deviation of the void fraction decreases significantly when the flow passes from probe CP1 to probe CP4 (just after the vena contracta of the orifice). Based on the flow pattern classification obtained in Fig.7, it appears that for a range of gas superficial velocities, there is a change of flow pattern from slug to bubbly and slug to churn flows when passing through the orifice. This can be confirmed by the decreasing in the void fraction values given by stars and plus symbols, except for the some highest values of gas superficial velocities where an increase in the void fraction is noticed. When passing to probe CP5 (Fig.7(b)), the standard deviation increases and becomes closer to that obtained from probe CP1, particularly at low and high gas superficial velocities. Unlike a significant changes in the flow regime transition between CP1 and CP4 found in Fig.7(a), very few changes in the flow regime (obviously at moderate gas superficial velocity, see Fig.7(b)) can occur between CP1 and CP5. This is due to the fact that the flow starts to recover at probe CP5.

For medium liquid superficial velocity, U_{ls}=0.58 m/s, same observations can be made, however with less decrease in standard deviation when passing from probe 1 to 4 than that for the lowest liquid superficial velocity. The flow is recovered approximately from probe CP5. One can also see that, the void fraction for probe CP1 and CP5 (Fig.7(d)) is almost same at low and moderate gas superficial velocities.

For the highest liquid superficial velocity U_{ls}=0.92 m/s at U_{gs}<0.7 m/s (Fig.7(e)), there is no change in the flow regime in which the standard deviation for CP1(upstream the orifice) and CP4(just after the contraction of the orifice) indicates that the flow is bubbly. For Ugs>0.7 m/s, it is clear that the standard deviation of the void fraction measured at CP1 shows slug flow while that at CP5 shows churn flow. In other words, beyond the gas superficial velocity of 0.7m the flow regime changed from slug flow upstream the orifice (i.e. at CP1) into churn flow when it passed through the orifice (i.e. at CP4). Same observations can be seen for probe CP5

(Fig.7(f)). However, less difference (gap) between CP1 and CP5 at U_{gs}<0.7 m/s can be noticed compare to that found in Fig.7(e).

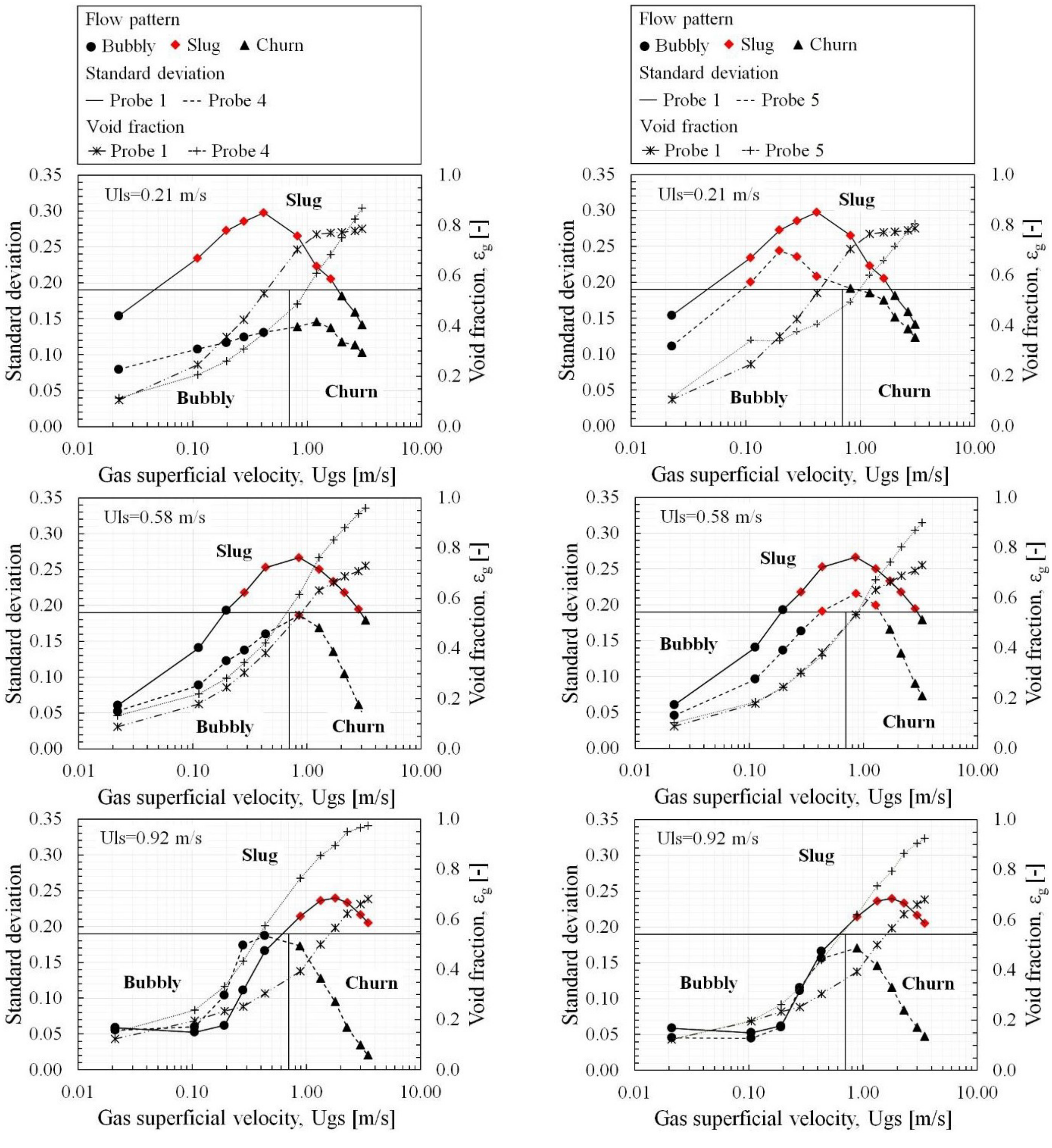

Fig.7. Void fraction and its Standard Deviation versus gas superficial velocity at Probes 1, 4 and 5, Uls=0.21, 0.58 and 0.92 m/s.

3.1.4 Slip ratio

Slip ratio parameter can be used to study the homogenization effect of the orifice in two-phase flows. It is defined as the ratio of the mean gas velocity, U_g to that of the liquid phase, U_L and can be written as;

$$S=\frac{U_G}{U_L} \qquad (2)$$

These mean velocities are related to the superficial gas and liquid velocities U_{gs} and U_{ls} respectively and the average void fraction, ε_g by

$$U_G=\frac{U_{gs}}{\varepsilon_g} \qquad (3)$$

And

$$U_L=\frac{U_{ls}}{1-\varepsilon_g} \qquad (4)$$

The slip becomes

$$S=\frac{U_G}{U_L}=\frac{U_{gs}(1-\varepsilon_g)}{U_{ls}\varepsilon_g} \qquad (5)$$

The variation of the slip ratio as a function of the mixture velocity ($U_M=U_{gs}+U_{ls}$) along the test section, using four orifices layouts is shown in Fig. 8(a)-(i). From these graphs, it appears that the type of the orifice significantly affects the relationship between the slip ratio and the mixture velocity. The slip ratio trends upstream the orifices are clearly different than those downstream the orifices (probes CP4, CP5 and CP6). In addition, if the variation of the slip ratio with mixture velocity at CP1 is compared to that at CP7, it would be seen that the slip ratio curves start to regain their initial trends from CP7 onwards. At probe CP4 (1D downstream the orifice Plate), and for each liquid superficial velocity used, it is seen that the slip ratio trends are different for all four orifice layouts. As the liquid superficial velocity increases, the slip ratio decreases, which indicates that increasing orifice holes number results in decreasing the slip ratio. In addition, at low-to-moderate mixture velocity, slip ratio increases monotonically. At probe CP5 (i.e. 3D downstream of the orifice), with a liquid superficial velocity equal to 0.58 m/s, the slip ratio is roughly unity for a wide range of mixture velocity indicating a good homogenization (mixing) effect of the orifice at this axial position. Further downstream, at probe CP6 (i.e. 7D downstream the orifice), at moderate to higher mixture velocity, the slip ratio becomes generally independent on the mixture velocity and it shows good mixing (homogenization) effect at higher liquid superficial velocity (U_{ls}=0.92) particularly, for nine-hole square layout where the slip ratio is almost unity. From this, one can conclude that the homogenization effect needs a minimum liquid superficial velocity of about 0.58 m/s (for the present study) to take place, and that the position of the good mixing or homogenization will depend on this critical minimum velocity as well as the orifice holes number.

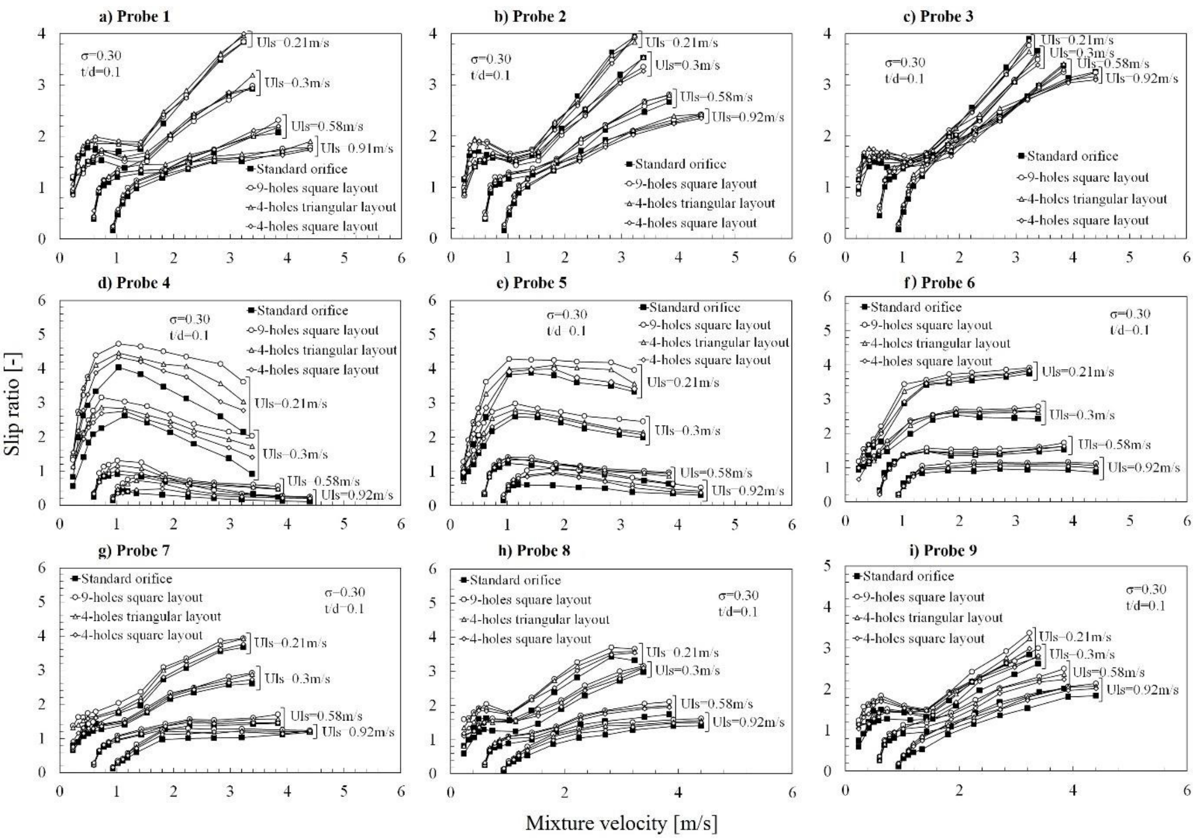

Fig.8. Relationship between slip ratio and mixture velocity along the test section for all orifices.

3.2 Pressure drop

3.2.1. Single-phase pressure drop

The dimensionless Euler number *Eu* which is commonly used to express the single-phase pressure drop Δp across the obstruction (e.g. single or multi-hole orifice) is given by:

$$Eu = \frac{\Delta p}{\rho U^2} \quad (6)$$

Where ρ is the density and U the is mean velocity. The range of the liquid velocity studied was 0 to 0.91 m/s. *Eu* is equivalent to 0.5 times the single-phase pressure drop coefficient, or resistance coefficient of the orifice, *k*.

Figure 9 shows the variation of the Eu with liquid Reynolds number ($\rho UD/\mu$, where D and μ are the pipe diameter and the viscosity respectively) for all four investigated orifices (see Table 1). It is obvious from the figure that Euler number is constant and it is almost independent of Reynolds number for all types of orifice plates. The standard orifice exhibits the highest Euler number (about 15), while the 4-holes square orifice gives the lowest Euler number (about 9). Euler numbers for the 9-holes square orifice and the 4-holes triangular orifice are approximately 10 and 12 respectively . This indicates that the Euler number (and thus the pressure drop across the orifice) is strongly dependent on the number of holes and their disposition across the orifice plate. Comparing 4-holes square orifice and 4-hole triangular orifice shows that the later offers higher pressure drop which means that, even at the same number of holes (with identical opening area), the shape of the holes has a significant influence on the pressure drop (and hence Eu). In addition, the response of 4-hole square orifice is very close to that for 9-hole square orifice indicating that the effect of increasing the number of the holes alone (providing that the shape of the holes for both orifices are identical) has less influence on the pressure drop across the orifice plate.

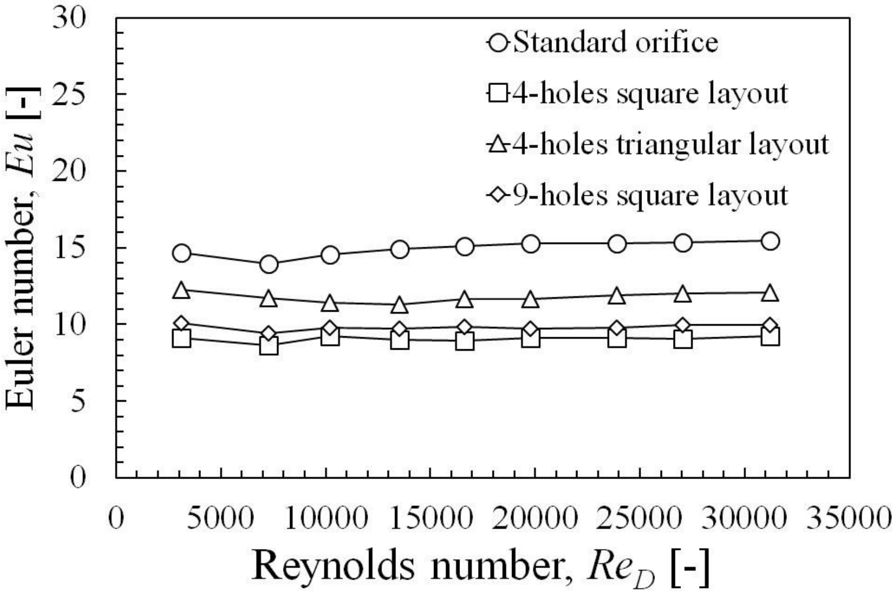

Fig.9. Effect of Reynolds number on Euler number using four orifice layouts

Models proposed in the literature for predicting single-phase pressure drop through single and multi-hole orifices i.e., the correlations of Idel'chick et al. [20], Mayens et al. [7] and Zhao et al. [6] are summarized in Table 2. The present data have been used to test the accuracy of these models. The results are shown in Fig.10. It appears from this figure that the predicted Euler number obtained from Idel'chik model (Fig.10(a)) is very similar to that estimated from Mayens et al. model (Fig.10(b)). Idel'chik model and Mayens et al. model showed that the estimated Euler number is almost under-predicted and the response of 4-hole square orifice and 9-hole square orifice offers minimum relative errors between predicted and experimental Euler number . Zhao et al. model showed that an estimated Euler number is over-predicted for all investigated orifices with minimum and maximum relative errors associated to standard orifice and 4-hole square orifice respectively.

Table 2: A summary of some existent models for predicting an Euler number for single-phase pressure drop through single and multi-hole orifices

Author	Euler number			
Maynes et al. [7]	$Eu=\frac{1}{2}\left[\left(\frac{A_p}{A_h}\right)^2\left(2-\frac{2}{\alpha}+\frac{2}{\alpha^2}\right)-2\left(\frac{A_p}{A_h}\right)+1\right]F(\emptyset)$	$F(\emptyset)=\begin{cases}2.9-3.65\emptyset+1.75\emptyset^2, & \emptyset\leq 0.95\\ 0.932+0.078\emptyset, & \emptyset>0.95\end{cases}$ $\emptyset=(t/d)(A_h/A_p)^{1/5}$		(7)
T. Zhao et al. [6]	$Eu=\frac{1}{2}P_m(EDR^{-4.448}-1)$ $Eu=\frac{1}{2}P_s(DR^{-4.187}-1)$	$P_m=160.325\left(\begin{array}{c}71.467EDR^4-100.3EDR^3\\+52.021EDR^2-11.801EDR+1\end{array}\right)$ $P_s=150.848\left(\begin{array}{c}74.679DR^4-103.507DR^3\\+53.001DR^2-11.874DR+1\end{array}\right)$		(8)
Idel'chick et al. [20]	$Eu=\frac{1}{2}\left[\left(\left(0.5+\tau\sqrt{1-\left(\frac{d}{D}\right)^2}\right)\left(1-\left(\frac{d}{D}\right)^2\right)+\left(1-\left(\frac{d}{D}\right)^2\right)^2+\lambda\frac{t}{d}\right)\left(\frac{D}{d}\right)^4\right]$		for $Re>10^5$	(9)
	$Eu=\frac{1}{2}\left[\left(\xi_\varphi+\varepsilon_0^{'Re}\xi_0+\lambda\frac{t}{d}\right)\left(\frac{D}{d}\right)^2\right]$		for $Re<10^5$	(10)
	$\xi_\varphi,\tau,\varepsilon_0^{'Re},\xi_0$ determined graphically, see Idel'chick			

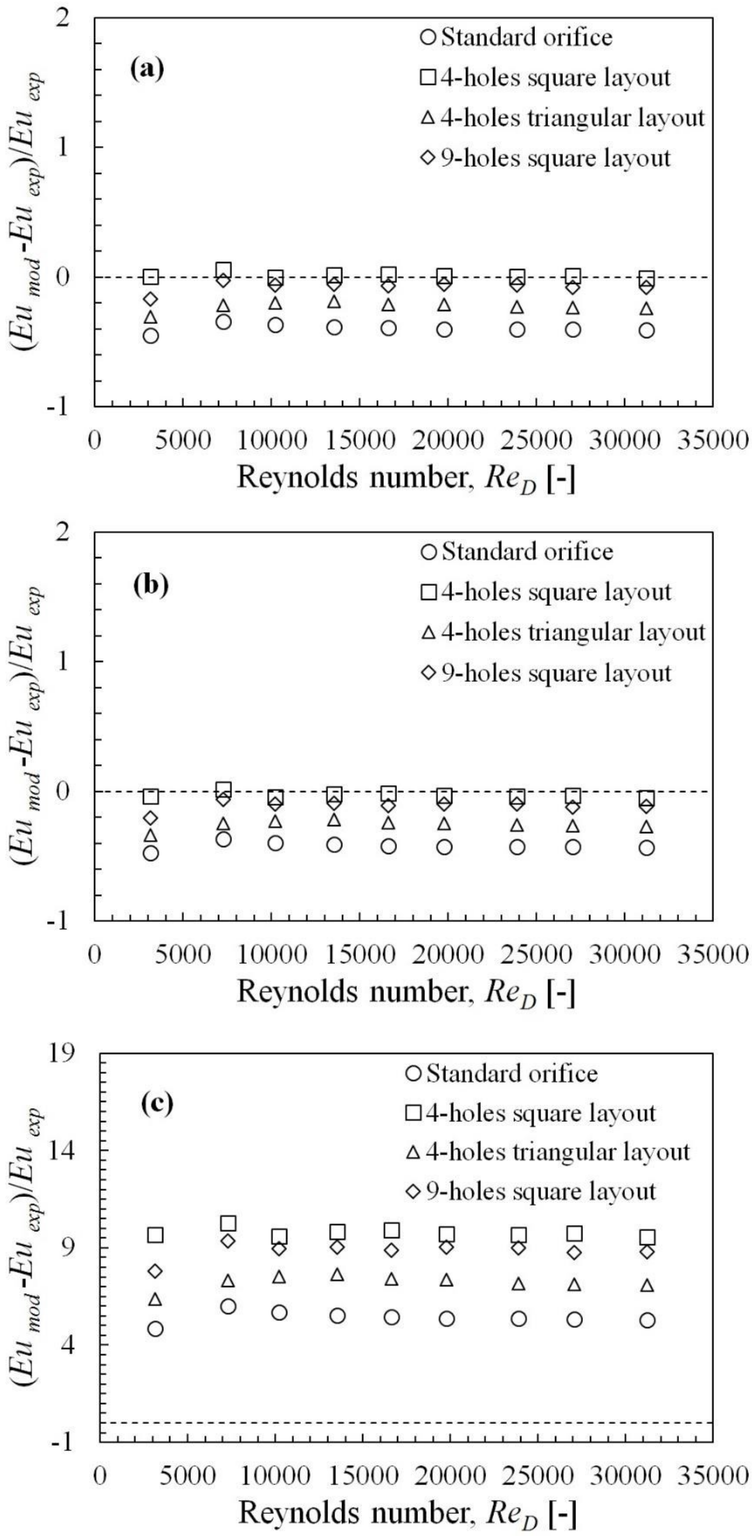

Fig.10. Relative error between predicted and experimental Euler number for single phase flow (a) Equations of Idel'Chick et al. [20]; (b) Equations of Maynes et al. [7], (c) Equations of Zhao et al. [6].

3.2.2. Two-phase flow pressure

3.2.2.1 Variation of upward two-phase pressure drop with gas superficial velocity through various layouts of orifice plates

Figure 11 displays the relationship between the pressure drop of upward two-phase flow through the four orifices and the gas superficial velocity, at different liquid superficial velocities. On this figure, error bars showing the uncertainties on the measurement as well as the flow pattern transition lines (e.g. bubbly to slug and slug to churn flows) are also plotted.

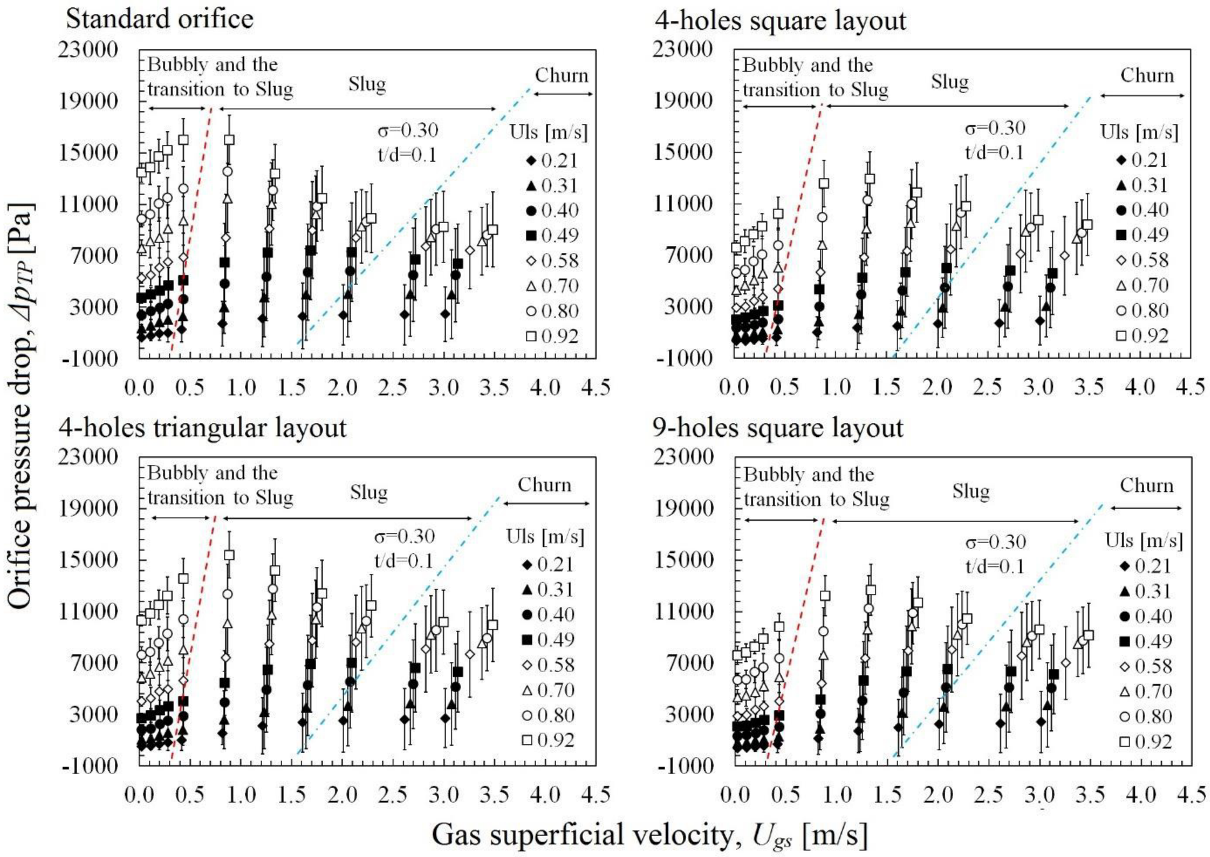

Fig. 11 Upward two-phase flow pressure drop versus gas superficial velocities at different liquid superficial velocities

It appears from these graphs that, qualitatively, the curves shows the same trends for all four orifices. Increasing number of holes and their positioning in orifice plates have a significant influence on the values of the two-phase flow pressure drop across these orifices. The standard orifice exhibits the highest pressure drop followed by 4-holes triangular layout, 4-holes square layout and 9-holes square layout respectively. Decreasing of the pressure drop with increasing the holes number is might be due to the uniformity in the flow and probably the vanishing of the vena contract. It is worth to remind that according to the work of Shannak et al. [21], on flow contraction in standard orifice, the vena contracta for the case of two-phase flow existed only for bubbly and annular flows.

in addition, the pressure drop is influenced by the flow regime in which the slope of the curves changes with changing flow regimes. when passing from a flow regime to another one.

For all investigated orifices, One can observe that four distinct regions of the pressure drop can be seen;

(i) at low gas superficial velocity (Ugs~<0.5 m/s) and full range of liquid superficial velocity (0.21m/s< U_{ls} < 0.92 m/s), where the pressure drop curves show positive steeper gradients.

(ii) at moderate gas superficial velocity (0.8m/s< U_{gs} < 2.2 m/s) and low-to-moderate liquid superficial velocity (0.21m/s< U_{ls} < 0.49 m/s), where the pressure drop curves indicate positive flatter slope.

(iii) at moderate gas superficial velocity (0.8m/s< U_{gs} < 2.2 m/s) and high liquid superficial velocity (U_{ls} > 0.49 m/s), where the pressure drop curves show steeper negative slope.

(iv) at high gas superficial velocity (U_{gs} >2.5 m/s) and full range of liquid superficial velocity (0.21m/s< U_{ls} < 0.92 m/s), where the pressure drop curves show flatter negative slope.

In conclusion, two general characteristics of the pressure drop across four investigated orifices are found. The first occurred at Uls <0.49m/s in which the trends of the pressure drop start with a steep positive slope at low gas superficial velocity, followed by a flatter positive slope at moderate gas flow and then negative slope at high gas superficial velocity. The second occurred at high gas liquid superficial velocity (Uls>0.49m/s) where the trends of the pressure drop start with a positive gradient at low gas superficial velocity followed by a steep negative slope and then flatter negative slope. The above discussion indicates clearly that three distinct flow regimes, in which the transitions between bubbly to slug and slug to churn flow, can be identified from the two-phase pressure drop across the orifices.

3.2.2.2 Assessment of the two-phase pressure drop correlations

Recently Zeghloul et al. [2], carried out an assessment of the two-phase flow pressure drop correlations in standard orifice and reported that those of Morris [22] and Simpson et al. [23] are the most reliable one. An assessment of these correlations along with the adapted one of Chisholm [24] and the homogeneous model is achieved in the present study. Table 3 summarizes these correlations.

Table 3: Two-phase flow pressure drop multiplier correlations for orifices.

Author	Correlation
Homogeneous	$\Phi^2_{LO}=1+x\,[\frac{\rho_l}{\rho_g}-1]$ (11)
Simpson et al. [23]	$\Phi^2_{LO}=[1+x(S-1)][1+x(S^5-1)]$; $S=(\frac{\rho_l}{\rho_g})^{1/6}$ (12)
Chisholm [24]	$\Phi^2_{LO}=1+(\frac{\rho_l}{\rho_g}-1)\,[Bx(1-x)+x^2]$ (13) Thin Orifice: $B=\frac{[\frac{1}{(C_c\beta)^2}-1]\frac{1}{S}-\frac{2}{C_c\beta S}+\frac{2}{S^{0.28}}}{\frac{1}{(C_c\beta)^2}-1-\frac{2}{C_c\beta}+2}$; Thick Orifice: $B=\frac{[\frac{1}{(C_c\beta)^2}-1]\frac{1}{S}-\frac{2}{C_c\beta^2 S}+\frac{2}{\beta^2 S^{0.28}}-[\frac{1}{\beta}-1]\frac{2}{S^{0.28}}}{\frac{1}{(C_c\beta)^2}-1-\frac{2}{C_c\beta^2}+\frac{2}{\beta^2}-\frac{2}{\beta}+2}$ $C_c=\frac{1}{[0.639(1-\beta)^{0.5}+1]}$ $S=\begin{cases}(1+x(\frac{\rho_l}{\rho_g}-1))^{0.5} & \text{if } X>1\\ (\frac{\rho_l}{\rho_g})^{\frac{1}{4}} & \text{if } X\leq 1\end{cases}$; $X=\frac{(1-x)}{x}(\frac{\rho_l}{\rho_g})^{0.25}$

Morris [22]	$\Phi^2_{LO} = [x\frac{\rho_l}{\rho_g} + S(1-x)]\,[x + (\frac{1-x}{S})\,(1 + \frac{(S-1)^2}{(\rho_l/\rho_g)^{0.5}-1})]$ S calculated in same manner as in Chisholm's equation	(14)

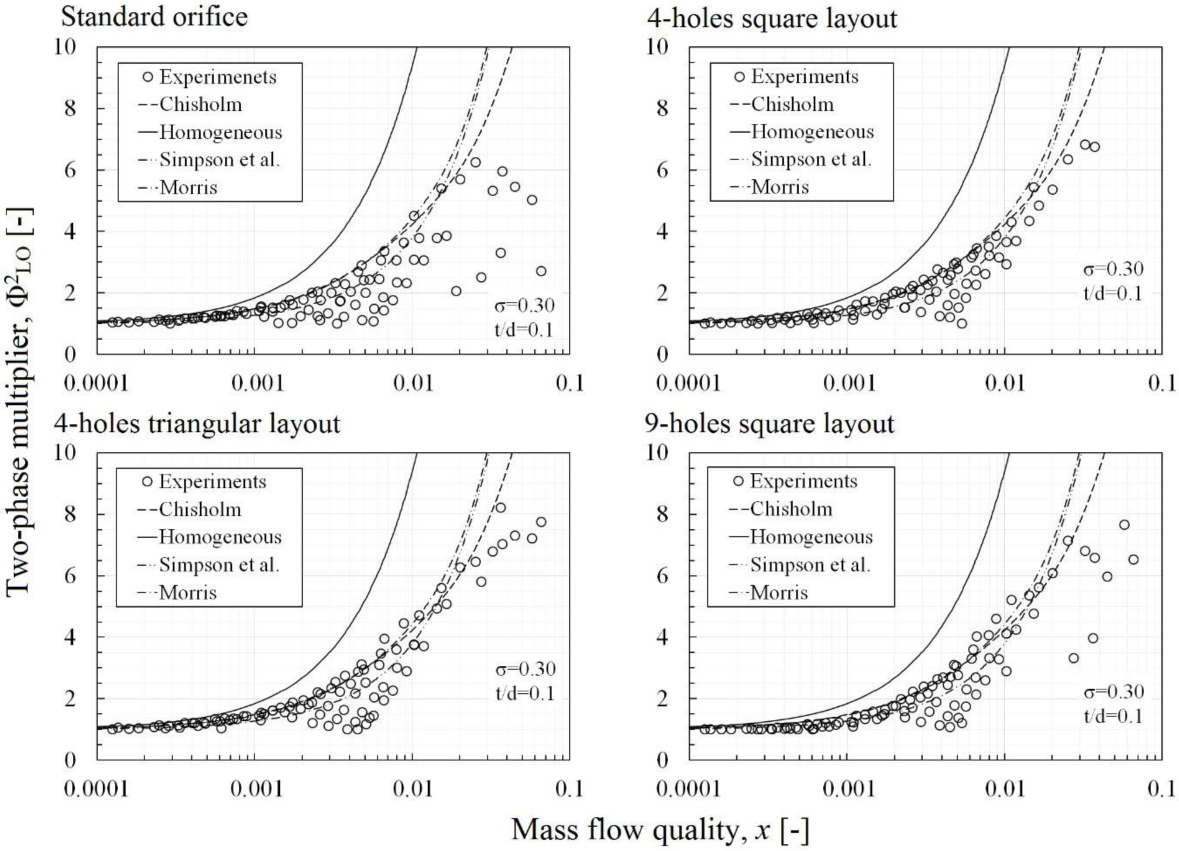

Fig. 12 Variation of experimental and predicted two-phase flow pressure drop multiplier with mass flow quality

Figure 12. Shows the comparison of the two-phase pressure drop obtained experimentally and those calculated by the models. For the standard orifice, the four models predict well the experimental data except the homogeneous model, which starts to over-predict the experimental values beyond a mass flow quality of 0.001indicating that, the homogenous flow model fits well with bubbly flow (i.e. at low gas superficial velocity) and breaks up beyond x=0.001. Same remarks can be reported for the four holes square and triangular layouts. For the nine holes orifice, the models slightly under-predict the pressure drop for low mass flow quality and

predict well the pressure drop for higher mass flow quality, except the homogeneous flow model which continue to over-predict greatly the experimental data.

In order to analyze further the accuracy of these models, plots of experimental data versus the theoretical pressure drop are shown in Figure 13. In addition, to quantify their accuracy the approach proposed by Govan [25] has been used. He carried out an assessment of the methods for comparing predictions and experimental data for large data sets and concluded that, rather than use an error, comparison should be made using the logarithm of the ratio of predicted to experimental values as this tends to yield a more Gaussian distribution. To judge the accuracy of the prediction methods, he proposed to use two statistical parameters, F and S. These are defined as: F, the correction factor, which is the average factor by which the calculated value must be multiplied to give the experimental value; and S which is a transformed standard deviation $= exp(\sigma)-1$, where ΔP_{mod} (i) is the predicted two-phase pressure drop and ΔP_{exp} (i) is the experimental two-phase pressure drop.

$$F=\frac{1}{exp(M)} \tag{15}$$

$$S=exp(R)-1 \tag{16}$$

$$\text{with: } M=\frac{1}{n}\sum_{i=1}^{n} e(i) \qquad e(i)=\log\left[\frac{\Delta P_{mod}(i)}{\Delta P_{exp}(i)}\right] \tag{17}$$

$$R=\sqrt{\frac{1}{n}\sum_{i=1}^{n}(e(i)-M)^2} \tag{18}$$

It is obvious from Figure 13, that the Homogeneous model over-predicts the pressure drop for the four orifices. This can be confirmed from Table 4, where the values of the factors F and S are far from unity and zero respectively. Equally for the standard orifice, the adapted correlation of Chisholm and the relationship of Morris predict well the pressure drop, however the predictions are better for multi-hole orifices with the values of F and S approaching unity and zero values respectively. The correlation of Simpson et al. predicts well the pressure drop for the whole orifices with values of F and S very close to unity and zero respectively.

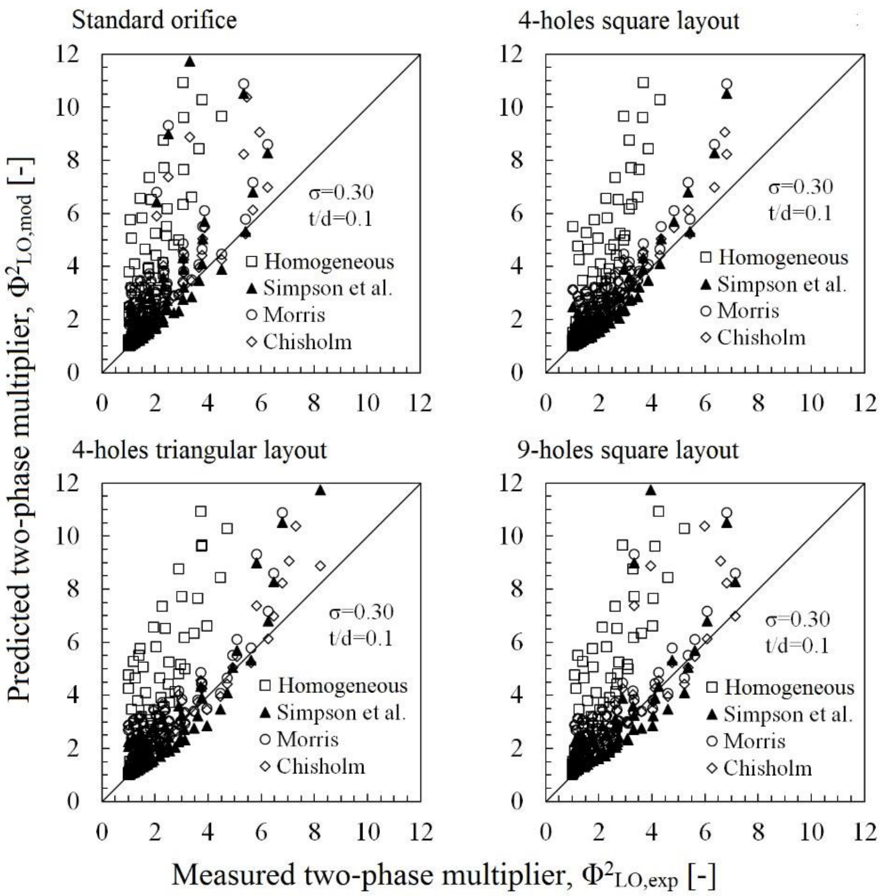

Fig.13. Comparison between measured and calculated two-phase flow pressure drop multiplier through orifices by models; Morris [22]; Simpson et al. [23]; Chisholm [24] and homogeneous flow model.

Table 4: Comparison of the experimental data with the selection of correlations.

Model		Standard orifice	4 - holes square layout	4 - holes triangular layout	9 - holes square layout
Homogeneous	*F*	0.725	0.791	0.770	0.759
	S	0.321	0.196	0.244	0.235
Chisholm [24]	*F*	0.861	0.922	0.916	0.903
	S	0.175	0.090	0.116	0.110
Morris [22]	*F*	0.850	0.917	0.904	0.891
	S	0.198	0.093	0.129	0.131
Simpson et al. [23]	*F*	0.919*	0.994*	0.977*	0.963*
	S	0.159*	0.085*	0.093*	0.098*

Conclusion

From the present work one can conclude that:

- ✓ Euler number for single phase flow was estimated and compared with three different models. It was well predicted by the correlations of Mayens et al. and Idel'chick et al where the response of 4-hole square orifice and 9-hole square orifice offers minimum relative error of Euler number.
- ✓ The void fraction was measured upstream and downstream the orifice at nine different axial locations. The flow is almost recovered after 7 D downstream the orifice plate.
- ✓ Following the work by Kaji et al. [19], a standard deviation threshold line of 0.2 was estimated to identify bubbly-to-slug and slug-to-churn flow transition regions.
- ✓ The type of the orifice has significant effect on the slip ratio downstream the orifice plate. As the liquid superficial velocity increases, the slip ratio decreases. In addition, increasing orifice holes number results in decreasing the slip ratio. At liquid superficial velocity equal to 0.58 m/s, the slip ratio was found to be unity for a wide range of mixture velocity at probe CP5 (i.e. 3D downstream of the orifice) which indicates a good homogenization effect.

- ✓ Two-phase pressure drop decreases with increasing the number of the holes in orifice plate. From two-phase pressure drop, three distinct regions were identified in which the slope of the trends changed significantly. These regions correspond to the bubbly to slug and slug to churn flow transition.
- ✓ The predicted two-phase flow multiplier showed that the correlation of Simpson et al. predicts well the pressure drop across the orifices.

NOMENCLATURE	
Ac	vena contracta area, m^2
A_h	Orifice hole area, m^2
A_P	pipe area, m^2
Cc	contraction coefficient ; $(\frac{4Ac}{\pi d^2})$
D	pipe diameter, m
D_d	the orifice distribution density
d_{hmin}	the minimum spacing between the orifices edges located at adjacent center circles
d	orifice diameter, m
e	logarithmic distribution error
F	Govan correction factor
g	acceleration of gravity, m/s^2
k	orifice resistance coefficient
K	the expansion factor
M	mean error
$\dot{m}$	mass flux, kg/m^2 s
n	the total orifice number
R	root mean square error
S	Tthe slip ratio (equation 12, 13 and 14)
S	Govan transformed standard deviation
S_D	the standard deviation
t	orifice thickness, m
U	the mean velocity
U_M	the mixture velocity, m/s
Ugs	gas superficial velocity, m/s
Uls	liquid superficial velocity m/s
x	mass flow quality; $(\frac{\dot{m}_g}{\dot{m}_g+\dot{m}_l})$
X	Lockhart-Martinelli parameter; $(\frac{\Delta P_l}{\Delta P_g})^{\frac{1}{2}}$
Y	the flow coefficient
Z	The axial distance from the orifice
Greek Letters	
β	diameter ratio of the orifice to that of the pipe; (*d/D*)
ΔP_{LO}	single-phase liquid pressure drop through orifice assuming total flow to be liquid, Pa
ΔP_{SP}	single-phase flow pressure drop through orifice, Pa
ΔP_{TP}	two-phase flow pressure drop through orifice, Pa
ε_g	void fraction or gas volume fraction; $(\frac{A_g}{A})$
$\varepsilon_0^{'Re}$	parameter of Idel'chick determined graphically
ζ	the pressure loss coefficient
ξ_φ	parameter of Idel'chick determined graphically

ξ_0	parameter of Idel'chick determined graphically
Φ^2_{LO}	two-phase flow pressure drop multiplier; $(\frac{\Delta P_{TP}}{\Delta P_{LO}})$
λ	friction factor
μ	dynamic viscosity, Pa s
ρ	fluid density, kg/m^3
σ	Orifice open area
α	Equartion de Maynes
τ	parameter of Idel'chick determined graphically
Non-Dimensional Numbers	
Eu	Euler number; $(\frac{\Delta P}{\rho U^2})$
Fr	Froude number
Re	Reynolds number; $(\frac{\rho U d}{\mu})$
Subscripts	
exp	experimental
g	Gas
l	liquid
LO	liquid only
mod	model
SP	single-phase
TP	two-phase flow
Abbreviations	
CP	The conductance probe
CFD	Computational Fluid Dynamics
DR	The diameter ratio of a single hole orifice
DP cell	Differential pressure transmitter
EDR	The equivalent diameter ratio of a multi-hole orifice
ERT	Electrical resistance tomography
GVF	The gas volume fraction
MOV	The multi-hole orifice valve
PVC	The mixer made of Polyvinyl chloride
V	Valve

REFERENCES

[1] **Muralidharan, V**. Response of a slotted plate flow meter to horizontal two-phase flow, MSc Thesis, Texas A&M University, 2003.

[2] **Zeghloul, A., Azzi, A., Saidj, F., Messilem, A., Azzopardi, B.J.** Pressure drop through orifices for single and two-phase vertically upward flow – implication for metering, Journal of Fluids Engineering, 2017, **139**, p 031302.

[3] **Kolodzie, P.A., Van Winkle, M.** Discharge coefficients through perforated plates, AIChE Journal, 1957, **3**, 305-312.

[4] **Gan, G., Riffat, S.B**. Pressure Loss Characteristics of Orifice and Perforated Plates, Experimental Thermal and Fluid Science, 1997,**14**, 160 165.

[5] **Testud, P., Moussou, P., Hischberg, A., Aurégan, A.** Noise generated by cavitation single-hole and multihole orifices in a water pipe. Journal of Fluids and structures, 2007,**23**, 163-189.

[6] **Zhao, T., Zhang, J., Ma, L. A**. General structural design methodology for multi-hole orifices and its experimental application, Journal of Mechanical Science and Technology, 2011, **25 (9)**, 2237-2246.

[7] **Maynes, D., Holt, G.J., Blotter, J**. Cavitation inception and head loss due to liquid flow through perforated plates of varying thickness, Journal of Fluids Engineering, 2013,**135** .

[8] **Barki, M., Ganesha, T., Math, M.C**. CFD analysis and comparison of fluid flow through a single hole and multi hole orifice, International Journal of Research in Advent Technology, 2014, **2 (8)**, 2321-9637.

[9] **Singh, V.K., Tharakan, T.J**. Numerical simulations for multi-hole orifice flow meter, Flow Measurement and Instrumentation, 2015, **45** , 375-383.

[10] **Morrison, G.L., Hall, K.R., Holste, J.C., Macek, M.L., Ihfe, L.M., Deotte, R.E., Terracina, D.P.** Comparison of orifice and slotted plate flow meters, Flow Meas. Instrum., 1994, **5** , 71-77.

[11] **Malavasi, S., Messa, G., Fratino, U., Pagano, A**. On the pressure losses through perforated plates. Flow Meas.Instrum., 2012, **28**, 57-66.

[12] **Morrison, G.L., Terracina, D., Brewer, C., Hall, K.R.** Response of a slotted orifice flow meter to an air/water mixture, Flow Meas. Instrum., 2001, **12**, 175-180.

[13] **Alimonti, C., Falcone, G., Bello, O**. Two-phase flow characteristics in multiple orifice valves, Exp. Therm. Fluid Sci. 2010, **34**, 1324-1333.

[14] **Geng, Y., Zheng, J., Shi, T**. Study on the metering characteristics of a slotted orifice for wet gas flow, Flow Meas. Instrum., 2006, **17**, 123-128.

[15] **Pirouzpanah, S., Çevik, M., Morrison, G.L**. Multiphase flow measurements using coupled slotted orifice plate and swirl flow meter, Flow Meas. Instrum. 2014, **40**, 157-161.

[16] **Annamalai, G., Pirouzpanah, S., Gudigopuram, S.R., Morrison, G.L**. Characterization of flow homogeneity downstream of slotted orifice plate in two-phase flow using electrical resistance tomography, Flow Meas. Instrum. 2016, **50**, 209-215.

[17] Zeghloul, A., Azzi, A., Saidj, F., Azzopardi, B.J. Hewakandamby, B. Interrogating the effect of an orifice on the upward two-phase gas-liquid flow behavior, Int. J. of Multiphase Flow, 2015, **74**, 96-105.

[18] International Organization for Standardization, Measurement of fluid flow by means of pressure differential devices, part1: orifice plates, nozzles and Venturi tubes inserted in circular cross-section conduits running full, ISO 5167-1, Geneva, (1991).

[19] **Kaji , R., Azzopardi, B.J., Lucas, D**. Investigation of flow development of co-current gas-liquid vertical slug flow, Int. J.of Multiphase Flow, 2009, **35**, 335-348.

[20] **Idel'chik, I., Malyavskayafs, G., Martynenko, O., Fried, E**. Handbook of Hydraulic Resistances, 3rd edition, 1994, CRC Press,.

[21] **Shannak, B., Friedel, L., Alhusein, M., Azzi, A**. Experimental investigation of contraction in single- and two-phase flow through sharp-edged short orifice, Forshung im ingenieurwesen, 1999, **64**, 291-295.

[22] S.D. Morris, Two-phase pressure drop across valves and orifice plates, in: European Two-phase Flow Group Meeting. Marchwood Engineering Laboratories, Southampton, UK, 1985.

[23] H.C. Simpson, D.H. Rooney, E. Grattan, Two-phase flow through gate valves and orifice plates. Int. Conf. Physical Modelling of Multiphase Flow, Coventry, 1983.

[24] D. Chisholm, Two-Phase Flow in Pipelines and Heat Exchangers, 1983, Longman Group Ed, London, 1983.

[25] A. Govan, A note on statistical methods for comparing measured and calculated values, United Kingdom Atomic Energy Authority Report AERE-M3621, 1988.